A two-layer detection model for infrared slow low-altitude targets

Jingli Gao
College of Electrical Engineering, *Zhejiang University*,
Hangzhou 310027, China
College of Software Engineering, *Pingdingshan University*,
Pingdingshan 467000, China

Chenglin Wen
School of Automation
Hangzhou Dianzi University
Hangzhou 310018, China
wencl@hdu.edu.cn

Meiqin Liu
College of Electrical Engineering
Zhejiang University
Hangzhou 310027, China
liumeiqin@zju.edu.cn

***Abstract*—This paper proposes a novel detection approach for dim targets with low signal-to-noise ratio in a image sequence. Initially, the superposition analysis is introduced to reveal the relationship between target energy and noise energy in the overlapped images, which is vital for the effectiveness of singular value decomposition, and also the relationship between signal-to-noise ratio and cosine angle of singular value vectors is analyzed, which illustrates the essence of angle-based detection methods. Second, analyzing the feasibility of locating targets using singular vectors, thus the first few singular vectors and threshold technology are combined to reconstruct the targets in each overlapped image, and then the positions of the suspected targets are connected to form tracks, which is validated in terms of Hough transform. Extensive experiments show that the proposed method not only works more stably under different signal-to-noise ratios, but also has better detection performance compared with the conventional baseline methods.**

***Index Terms*—low-altitude, cosine angle, singular vector location, target detection**

I. Introduction

With the plethora and wide application of unmanned aerial vehicles, model airplanes, gliders and delta wings and other slow low-altitude small targets, the accurate detection of these targets and thus effective supervision have become the difficult problem of air defense security and research focus [1]. The slow low-attitude targets are usually buried in heavy noises, and have no effective shape and texture because of small sizes, though are obtained from near distance imaging. Therefore, it is extremely difficult to separate them from the heavy noise. In reality, most targets in the low-altitude airspace are subject to slow movement. As such, the detection of slow low-altitude targets has received extensive attention in the past few years [1], [2].

The traditional track before detect (TBD) methods, such as Hough transform (HT) [3], matched filter [4], hypothesis testing [5], dynamic programming [6], [7], spatial-temporal bilateral filter [8], spatial-temporal local contrast filter [9], are proposed to detect fast moving targets measured from the long imaging distance, such as anti-ship missiles and high speed aircrafts, or deal with the case where the targets are stationary most of the time but the detection platforms could move fast, such as airplane-based and missile-based systems. As a whole, the TBD methods mainly rely on specific knowledge of target shape and velocity, which might be difficult to retrieve in real applications. Therefore, these methods are not always helpful in directly detecting slow low-altitude targets.

The detect before track (DBT) methods perform well for small targets with high signal-to-noise ratios (SNRs), such as sparse representation based on discriminative over-complete dictionary [10], multi-directional composite window [11], angle of singular value vectors [12], differences of neighboring singular values [13], infrared patch-image (IPI) models [14]–[16], weighted local difference measure [17], multiscale patch-based contrast measure [18]. However, for small targets with low SNRs, the detection performance could degrade rapidly.

In this paper, we propose a two-layer detection approach for slow small dim targets. First, the superposition method is used to accumulate the energy of weak targets, the rapid frame rate and slow moving property make the superposition method a powerful tool for energy accumulation. Second, the cosine angles caused by difference characteristics between normal and abnormal singular value vectors is used for the first-layer detection. Third, in the second-layer detection, the suspected targets are obtained by singular vector localization and threshold technology, and the target trajectories are obtained in terms of target association and validated according to Hough transform. The first advantage of usage of SVD in the proposed method is the whole detecting ability based on singular values, and the second advantage is the local detecting ability based on singular vector locating. The main contributions of this paper are summarized as follows: (1) analyze the influence of residual image superposition on signal-to-noise ratio, and reveal the relationship between signal-to-noise ratio and cosine angle. These two aspects form the basis for cosine angle detection. (2) propose a weak target detection approach based on singular vector locating and target association.

The remainder of this paper is organized as follows. Section II describes the first-layer detection method based on cosine angles of singular value vectors and the second-layer detection method based on singular vector localization and target association. Section III shows extensive synthetic experimental results and discussions. Conclusions are given in Section IV.

This work was supported by the National Natural Science Foundation of China (U1509203,61503206,61333005), the Zhejiang Provincial Natural Science Foundation of China (LZ16F030002), and the Aerospace Science Foundation of China (2015ZC76006).

II. Two-layer target detection model

A. Target observation model

Since the background scene changes quite slowly, thus several background images can be averaged as the background template. After subtracting the background template from each image, the residual image can be modeled as [19]

$$X_r(x,y,j) = D(x,y,j) + N(x,y,j) \tag{1}$$

where $X_r(x,y,j), D(x,y,j)$ and $N(x,y,j)$ denote the intensity of the pixel at coordinate (x,y) in the jth residual image, target image and noise image respectively, and $N(x,y,j)$ follows the standard normal distribution.

According to the residual image model described in formula (1), the superimposed image in the temporal domain can be expressed as the sum of two parts

$$X^k(x,y) = D^k(x,y) + N^k(x,y) \tag{2}$$

where $X^k(x,y) = \frac{1}{k}\sum_{j=1}^{k} X(x,y,j)$, $D^k(x,y)$ denotes the overlapped target image and $D^k(x,y) = \frac{1}{k}\sum_{j=1}^{k} D(x,y,j)$, and $N^k(x,y) = \frac{1}{k}\sum_{j=1}^{k} N(x,y,j)$ and $N^k(x,y)$ denotes the overlapped noise image. Define the ratio of the overlapped area of targets in adjacent images as the overlap degree olp, which is denoted by the expression of the parameter t [19]. The decay rate of the overlapped noise image is denoted by ρ_k^N, and the decay rate of the overlapped target image is denoted by $\rho_{k,l}^D$, where k is the overlap times, and l denotes different overlapping situation. Suppose that the target has a size of $m \times n$, and has constant intensity d. The size of the t The abnormal degree of an image is defined as the ratio of target energy to noise energy, and denoted by abd.

B. First-layer target detection

1) Influence of superposition of residual images on signal-to-noise ratio: In [19], it is pointed out that, (1) when $olp = 1$, $\rho_{k,1}^D = 1$; (2) when $olp = 0$, $\rho_{k,2}^D = k$; (3) when the target moves along the lines which are parallel to any axis, and $olp = \frac{1}{t}$, $\rho_{k,3}^D = \frac{tk^2}{(t+2)k-2}$; (4) when the target moves along the lines which are parallel to any axis, and $olp = \frac{t-1}{t}$, $\rho_{k,4}^D = \frac{3k^2}{3kt-t^2+1}$; (5) the decay rate of the overlapped noise image satisfies $\rho_k^N > k$. However, the case is not considered when the target moves along the lines which are not parallel to any axis.

When the target moves along the diagonal line direction, and $olp = \frac{(t-1)^2}{t^2}$, the energy of the overlapped target image can be expressed as

$$E_{D^k} = \frac{-t^3 + 4kt^2 + t + 2k}{6tk^2} mnd^2$$

where $t \geq 2$ and $k \geq t$, then the decay rate ρ_k^D of the overlapped target image can be computed as

$$\rho_{k,5}^D = \frac{E_{D^1}}{E_{D^k}} = \frac{6tk^2}{-t^3 + 4kt^2 + t + 2k} \tag{3}$$

When the target moves along the diagonal line direction, and $olp = \frac{1}{t^2}$, the energy of the overlapped target image can be expressed as

$$E_{D^k} = \frac{kt^2 + 2k - 2}{k^2t^2} mnd^2$$

where $t \geq 2$ and $k \geq t$, then the decay rate ρ_k^D of the overlapped target image can be computed as

$$\rho_{k,6}^D = \frac{E_{D^1}}{E_{D^k}} = \frac{k^2t^2}{kt^2 + 2k - 2} \tag{4}$$

When choosing a proper value for parameter t, it can be proved that

$$\frac{t-1}{t} > \frac{(t-1)^2}{t^2} > \frac{1}{t} > \frac{1}{t^2} \tag{5}$$

thus

$$\rho_{k,1}^D < \rho_{k,4}^D < \rho_{k,5}^D < \rho_{k,3}^D < \rho_{k,6}^D < \rho_{k,2}^D < \rho_k^N \tag{6}$$

From inequality (6), we can conclude that the energy decay rate is inversely proportional to the overlap degree, and the energy of the overlapped noise image N^k decays faster than that of the overlapped target image D^k after superposition. Thus the ratio of the energy of the overlapped target image to the energy of the overlapped noise image is increasing through superposition operation, which provides the theoretical basis for feasibility of target detection.

2) Relationship between signal-to-noise ratio and cosine angle: As mentioned above, the overlap of residual images could change the signal-to-noise ratio of the final overlapped image, which in fact leads to a jump in the singular values of the image. Hence an angle could occur between the exceptional singular value vector containing jumps and other normal singular value vector. Therefore, considering the relationship between the angle and signal-to-noise ratio in more detail is vital to target detection. The abnormal degree here is used to indicate the signal-to-noise ratio [19].

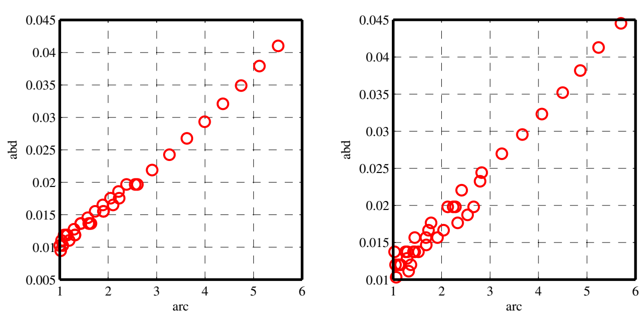

(a) (b)

Fig. 1. cosine angles vs. abnormal degrees

On the one hand, we assume that the intensities of the target pixels in an image sequence vary from 1 to 36 successively, and each intensity value corresponds to one image. For each image, increase the target area, and then calculate the abnormality when the target can be detected in terms of the cosine angle threshold. As can be seen from Fig. 1(a), when the target in each image can be detected, the abnormal degree is proportional to the angle computed by cosine angle rule. On the other hand, we assume that the target areas in an image sequence vary from 1 to 36 successively, and each target area corresponds to one image. For each image, increase the intensity of the target, and then calculate the abnormality when the target can be detected in terms of the cosine angle threshold. As can be seen from Fig. 1(b), when the target in each image can be detected, the abnormal degree is also proportional to the angle computed by cosine angle rule.

As discussed above, it can be concluded that the cosine angle could increase with the increasing abnormal degree. Hence the cosine angle can be used to detect small targets in an image.

3) Target detection based on superposition and cosine angle: The proposed first-layer target detection algorithm is described as follows:

- Step 1: Obtain the superimposed residual image X^k and the normal residual image $\overline{X}$ which does not contain any target.
- Step 2: Perform SVD on image X^k and $\overline{X}$ respectively, here s and $\overline{s}$ denote the singular value vectors of X^k and $\overline{X}$ respectively.
- Step 3: Compute the angle θ between s and $\overline{s}$. If $\theta \geq \gamma$, then it is certain that there must be a target in the test image, where γ is a threshold determined experimentally.

C. Second-layer target detection

1) Location analysis based on singular vectors: In [12], it is pointed out that the singular vector itself necessarily reflects the defect features when the image is defective, and the larger components of left singular vector indicates the defect range in the vertical direction, while the larger components of right singular vector indicates the defect range in the horizontal direction, regardless of component signs.

In fact, there are also similar observations in the target detection. For an image, the components of a singular vector with different signs may indicate different patterns, and the components with larger absolute values correspond to salient patterns, which could be merged into suspected targets.

2) Target association based on singular vector reconstruction: Combining superposition operation and singular vector reconstruction, we could get as many target patterns in an image as possible with low level false alarms. However, the false alarms in the reconstruction image could not be completely removed, and it is difficult to distinguish false alarms from weak targets with several pixels in a single image due to the fact that they have similar size or intensities. It is well known that compared with false alarms, a moving target in several continuous frames could form a trajectory. So it is the big difference between false alarms and real targets, and thus the obtained target trajectories could be used to determine real targets. Below is the process to associate suspected targets based on singular vector reconstruction.

For a target with size 3×3 in an image, Fig. 2 illustrates some typical target patterns obtained by singular vector reconstruction. Except the leftmost pattern, the remains contain only part of 3×3 pixels. For targets consisting of few pixels as in shown in Fig. 2, it is difficult to directly compute their correct central positions. Thus the dilation operation is required to form whole compact targets.

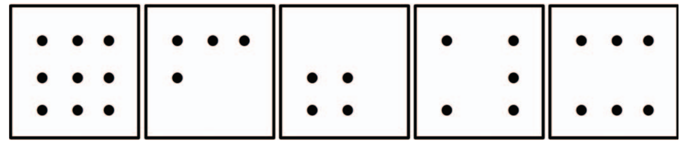

Fig. 2. Representatives of reconstructed targets

After dilation operation, we can get enlarged compact targets which could be used to compute the central positions more precisely than using the original targets. Then the computed positions are used to form target trajectories. If there are several targets in a single image, and the targets could be distinguished by the distance between each other, we could use the distances between the positions obtained from the current frame and the positions computed from the next frame to associate different targets.

3) Target detection based on superposition and target association: The proposed second-layer detection algorithm is described as:

- Perform SVD on the superimposed residual image X^k, process the left and right singular vectors by a thresholding operator, and then obtain reconstructed image $\hat{X}$ with the modified singular vectors.
- Apply the morphologic operator to connect the isolated pixels of suspected targets together, and form whole compact targets.
- Process suspected targets to obtain target trajectories. If a trajectory could be obtained, then it is certain that a target exists in an image sequence.

III. Experiments

A. Experimental setup

Experiments are performed on several synthesized image sequences, and each image X_r in an image sequence could be obtained by adding a target image D and a noise image N in the following way

$$X_r(x, y) = D(x, y) + N(x, y)$$

where $x \in [x_0 + 1, x_0 + m]$ and $y \in [y_0 + 1, y_0 + n]$, (x_0, y_0) is the coordinate of a point randomly selected from image X_r, $N(x, y)$ follows standard normal distribution, and if $x \in [x_0 + 1, x_0 + m]$ and $y \in [y_0 + 1, y_0 + n]$, $D(x, y) \neq 0$, otherwise $D(x, y) = 0$, and the image D would be blurred by a Gaussian filter to make it close to a real infrared image. Note that the superimposed residual image is obtained according to (2) through the sliding window technology.

In the first-layer detection, the detection results are evaluated by comparing the computed cosine angles with the predefined threshold. The detection performance based on cosine angle can be evaluated by the detection probability P_d.

$$P_d = \frac{\#\ number\ of\ true\ detections}{\#\ number\ of\ images} \tag{7}$$

In the second-layer detection, the detected target positions are compared with the true target positions obtained manually from the test sequences. For each sequence, the tolerance rectangles are $(\pm 6, \pm 6)$ pixels around the central positions. The detection probability P_t and false alarm rate F_t based on singular vector reconstruction are applied to evaluate the detection results [20].

$$P_t = \frac{\#\ number\ of\ true\ positions}{\#\ number\ of\ true\ targets} \tag{8}$$

$$F_t = \frac{\#\ number\ of\ false\ positions}{\#\ number\ of\ images} \tag{9}$$

B. Detection results

1) Influence of parameters: For the first-layer detection, we make 10000 times test to evaluate the parameter γ. In each test, first generate two images whose pixels follow the standard normal distribution, then compute the cosine angle between their singular value vectors. As shown in Fig. 3(a), the computed cosine angles range from 0.31 to 0.75, 93.4 percent of them are less than 0.55. Therefore, 0.55 could be a good choice for γ, which is just an evidence that there may exist targets in the test image.

For the second-layer detection, suppose that, there are 240 frames in the test sequence, three targets are moving with horizontal velocities, specified in pixels per frame (p/f), that is, $v_x = 1.0$ p/f and $v_y = 0$ p/f and the length of sliding window k equals one, that is, the superposition operation is not used here. Each target has SNR value of about 1.86, and size of 6×6. The parameter ρ here denotes the accumulative contribution rate and takes values from $[0.01, 0.05, 0.09, \cdots, 0.93, 0.97, 1]$, the parameter δ determines the structruing element radius and takes values from $[1, 2, 3]$. Another key factor is the shape of structure element. The receiver operating characteristic (ROC) curves can be computed by setting some parameters and by varying another parameter.

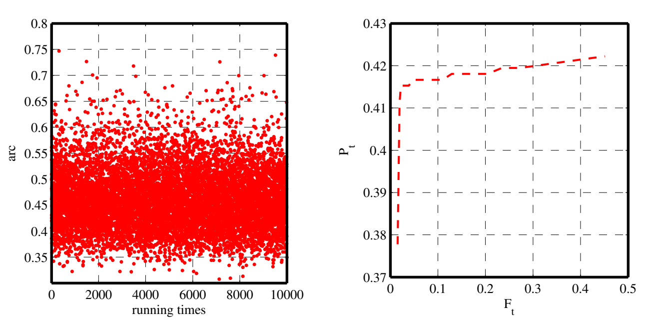

(a) (b)

Fig. 3. (a) Cosine angles for different running times, (b) ROC curve for different ρ

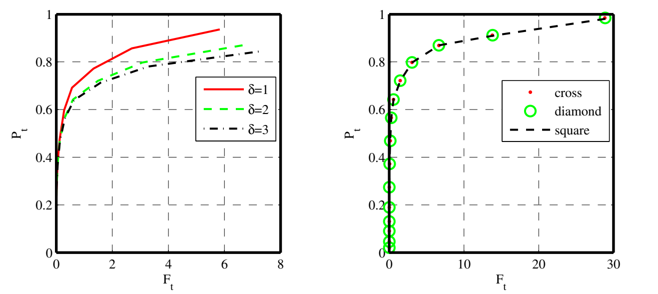

(a) (b)

Fig. 4. Comparison results of (a) different radius, (b) different dilation element.

The ROC curve shown in Fig. 3(b) can be computed by varying ρ each time. It can be concluded from Fig. 3(b) that the tracking probability P_t mainly benefit from the first few singular vectors, and is less dependent on the remaining singular vectors. When the value of parameter ρ exceeds 0.17, the tracking probability P_t could not be improved much.

Each δ corresponds to a ROC curve in Fig. 4(a). When the radius becomes bigger, the size of the target after dilation operation could become larger or two true targets could be merged together. This could cause less true targets to be located in the given tolerance rectangle. Thus the detection performance become worse.

As shown in Fig. 4(b), for a fixed radius, three different classes of elements with the same fixed radius are likely to have a similar effect on the detection performance, because the central positions computed by using these different elements are almost the same for a target.

2) Comparison to other methods: We use several sequences to test the proposed two-layer method and other methods. The detailed features of these sequences are listed in Table I. In Fig. 5, the rows from top to bottom of (i) or (ii) correspond to the detection results using the TopHat, Median, Mean and proposed method respectively. From Fig. 5(d)-(h), we can find that the initial superimposition step can obviously improve the detection results of the four test methods compared with the detection result of Fig. 5(c), because it benefits much from the slow movement of targets, which helps to enhance signal-to-noise ratio of targets after superimposition, thus the preprocessing step is necessary for almost all weak target detection tasks. Columns 2 to 9 of Table II in turn are the detection probability P_t and false alarm rate F_t of the TopHat, Median, Mean and proposed method, and Columns 10 to 11 are the detection probability P_d and trajectory number respectively. From Table II, we can find that the proposed method has better detection performance compared with the Median, Mean and TopHat methods, and the TopHat method has the worst performance, especially bad for very weak targets. Fig. 6 shows the target trajectories obtained by the proposed method on Seq 5, Seq 6, Seq 7 and Seq 8 respectively. Note that the overlap times k for Seq 5, Seq 6, Seq 7 and Seq 8 are 20, 40, 40, and 6 respectively. As can be seen from Fig. 6(c)-(e),

TABLE I
DETAILS OF DIFFERENT IMAGE SEQUENCES.

Sequences	Target details per frame				Frame details	
	SNR	size	num	(v_x, v_y) (p/f)	size	num
Seq 1	2.33	6×6	1	(1,0)	256×256	240
Seq 2	0.93	6×6	1	(1,0)	256×256	240
Seq 3	1.49	6×6	1	(1,1)	256×256	240
Seq 4	2.98	6×6	1	(1,0.1)	256×256	240
Seq 5	1.95,1.49,2.42	6×6	3	(1,0.1),(1,0),(1,0.2)	256×256	240
Seq 6	0.93,1.67,2.05	6×6	3	(1,0.08),(1,0),(1,0.05)	256×256	240
Seq 7	0.74,1.12,0.56	6×6	3	(1,0),(1,0),(1,0)	256×256	240
Seq 8	1.12,1.49	6×6	2	(0.2,0.5),(0.6,0.1)	256×256	240

although the superposition operation could help to enhance the weak targets, it is difficult to obtain correct detection results due to short trajectory information. However, as the target trajectories become longer as shown in Fig. 6(f)-(h), Hough transform could be used to determine the true trajectories. Although some targets could not be located in some frames due to noises or threshold selection, such as Fig. 6(g), the obtained tracks suggest the existence of three targets in Seq 7.

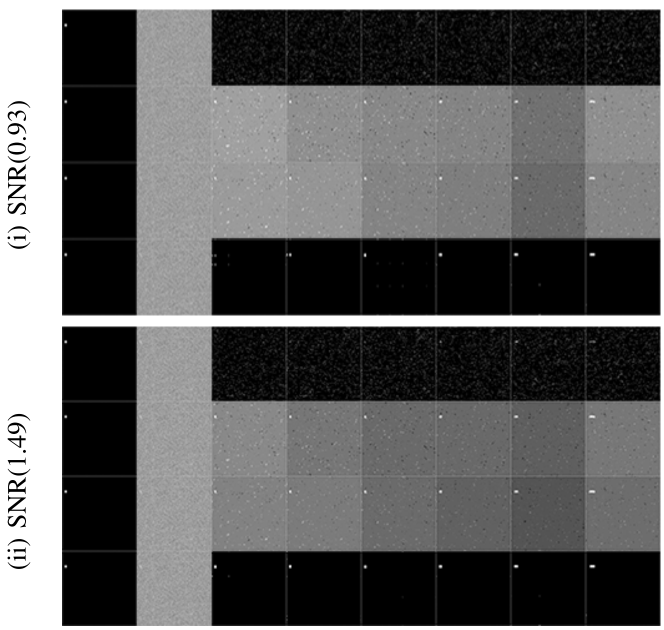

Fig. 5. Detection results of superimposed images in (i)(Seq 2) and (ii)(Seq 3) using the TopHat, Median, Mean and proposed method: (a) initial reference target, (b) single input image, detect results of (c) single input image, (d) stacking two consecutive images, (e) stacking three consecutive images, (f) stacking six consecutive images, (g) stacking twelve consecutive images, (h) stacking nineteen consecutive images.

IV. CONCLUSION

A two-layer detection model for a class of slow dim targets is presented based on superposition, cosine angle, singular vector locating and target association. First, the superposition is required before performing SVD, in order to increase the ratio of the target energy to the noise energy in the overlapped residual images. Then, the slow dim target detection is

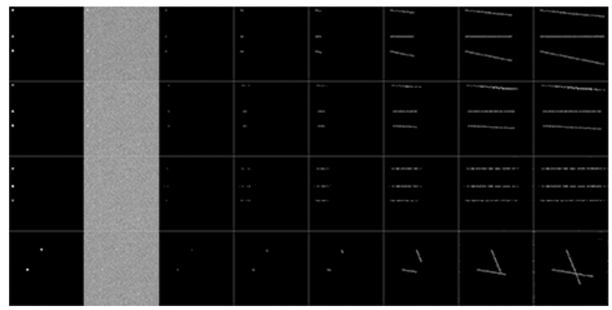

Fig. 6. Target trajectories obtained by the proposed method on Seq 5, Seq 6, Seq 7 and Seq 8: (a) initial reference target, (b) single input image, tracking results of (c) images k to $(k+3)$, (d) images k to $(k+10)$, (e) images k to $(k+20)$, (f) images k to $(k+80)$, (g) images k to $(k+160)$, (h) images k to 240.

transformed into a two-layer detection task, which is fulfilled by computing cosine angles and forming target tracks. The evidence chain obtained through two-layer detection are more confident that the detection results are optimal. Extensive synthetic experiments show that the proposed method can work stably from low SNR targets to high SNR targets (from seq 1 to seq 8), not only can detect interested targets with evidence chain, but also can give the target number in an image sequence more precisely in terms of trajectories.

REFERENCES

[1] Wang Z, Yan M A, Wang L R. Assessment of Threat Degree for LSS Target in Air Defense Operation[J]. Shipboard Electronic Countermeasure, 2013.
[2] Zhang J W, Guo H M. Net cast interception system research aimed at low small slow target[J]. Computer Engineering & Design, 2012, 33(7):2874-2878.
[3] Falconer D G. Target tracking with the Hough transform[C]. 1977 11th Asilomar Conference on Circuits, Systems and Computers, 1977. Conference Record. IEEE, 1977: 249-252.
[4] Reed I S, Gagliardi R M, Stotts L B. Optical moving target detection with 3-D matched filtering[J]. IEEE Transactions on Aerospace and Electronic Systems, 1988, 24(4): 327-336.
[5] Blostein S D, Huang T S. Detecting small, moving objects in image sequences using sequential hypothesis testing[J]. IEEE Transactions on Signal Processing, 991, 39(7): 1611-1629.
[6] Arnold J, Shaw S W, Pasternack H. Efficient target tracking using dynamic programming[J]. IEEE Transactions on Aerospace and Electronic Systems, 1993, 29(1): 44-56.
[7] Barniv Y. Dynamic programming solution for detecting dim moving targets[J]. IEEE Transactions on Aerospace and Electronic Systems, 1985 (1): 144-156.

TABLE II
COMPARISON RESULTS OF DIFFERENT METHODS UNDER DIFFERENT IMAGE SEQUENCES.

	TopHat		Median		Mean		proposed			
	P_t	F_t	P_t	F_t	P_t	F_t	P_t	F_t	P_d	Num of trajectories
Seq 1	0.97	116.34	1.0	81.28	1	83.35	1.0	0.02	1.0	1
Seq 2	0.40	116.02	0.96	91.12	1.0	96.89	1.0	0.02	1.0	1
Seq 3	0.70	116.04	1.0	88.08	1	92.75	1.0	0.08	1.0	1
Seq 4	1.0	115.08	1.0	74.88	1.0	74.79	1.0	0.05	1.0	1
Seq 5	0.88	38.76	1.0	22.74	1.0	22.26	1.0	0.13	1.0	3
Seq 6	0.68	38.68	0.98	25.21	1.0	25.35	0.86	0.42	1.0	3
Seq 7	0.27	38.55	0.80	29.30	0.88	30.85	0.84	0.72	1.0	3
Seq 8	0.54	57.94	0.99	42.41	1.0	44.19	1.0	0.13	0.8	2

[8] Bae T W. Spatial and temporal bilateral filter for infrared small target enhancement[J]. Infrared Physics & Technology, 2014, 63(2):42-53.

[9] Deng L, Zhu H, Tao C, et al. Infrared moving point target detection based on spatialtemporal local contrast filter[J]. Infrared Physics & Technology, 2016, 76:168-173.

[10] Li Z Z, Chen J, Hou Q, et al. Sparse Representation for Infrared Dim Target Detection via a Discriminative Over-Complete Dictionary Learned Online[J]. Sensors, 2014, 14(6): 9451-9470.

[11] Yang X, Zhou Y, Zhou D, et al. A new infrared small and dim target detection algorithm based on multi-directional composite window[J]. Infrared Physics & Technology, 2015, 71: 402-407.

[12] Gao J, Wen C, Liu M. steel surface defect detection and localization based on SVD and two-side compressive measurements[C]. The 26th Chinese Control and Decision Conference, May31-June 2, 2014: 1401-1406.

[13] Gao J, Wen C, Liu M. SVD-based scattered small targets detection[C]. 2014 International Conference on Multisensor Fusion and Information Integration for Intelligent Systems (MFI). IEEE, 2014: 1-6.

[14] Gao C, Meng D, Yang Y, et al. Infrared Patch-Image Model for Small Target Detection in a Single Image[J]. IEEE Transactions on Image Processing A Publication of the IEEE Signal Processing Society, 2013, 22(12):4996-5009.

[15] Dai Y, Wu Y, Song Y. Infrared small target and background separation via column-wise weighted robust principal component analysis[J]. Infrared Physics & Technology, 2016, 77:421-430.

[16] Wang C, Qin S. Adaptive detection method of infrared small target based on target-background separation via robust principal component analysis[J]. Infrared Physics & Technology, 2015, 69:123-135.

[17] Deng H, Sun X, Liu M, et al. Small Infrared Target Detection Based on Weighted Local Difference Measure[J]. IEEE Transactions on Geoscience & Remote Sensing, 2016, 54(7):4204-4214.

[18] Wei Y, You X, Li H. Multiscale patch-based contrast measure for small infrared target detection[M]. Pattern Recognition, 2016, 58: 216226.

[19] Gao J, Wen C, Liu M. Low-speed small target detection based on SVD and superposition. Journal of Shanghai Jiao Tong University, 2015(6): 876-883.

[20] Gao C, Meng D, Yang Y, et al. Infrared patch-image model for small target detection in a single image[J]. IEEE Transactions on Image Processing, 2013, 22(12): 4996-5009.